

ON RADIATIVE TRANSPORT OF THE RESONANCE LINES OF SODIUM

J. HUENNEKENS and T. COLBERT

Department of Physics, Lehigh University, Bethlehem, PA 18015, U.S.A.

(Received 15 July 1988)

Abstract—In this work, we discuss the effects of incomplete frequency redistribution on radiation trapping of the sodium D lines in laboratory experiments. We compare measured radiative escape factors from two recent experiments with values calculated from the Holstein theory, which assumes complete redistribution, and the Post theory, which explicitly takes into account both incomplete redistribution and the hyperfine structure of the atom. We show that the upturn of the escape factor vs density curve reported in the experiments of Romberg and Kunze is not a manifestation of the effects of incomplete redistribution. We also show that the data of Huennekens and Gallagher are more accurately fitted by a simple Holstein theory expression, where all effects of natural broadening on the lineshape are ignored, than by the more complete Post theory calculations. This is due to the fact that, in the present case, the density region where trapping is affected by incomplete frequency redistribution is small. Other recent experiments in mercury by Post and coworkers have demonstrated that such effects can be significant under different conditions. In addition, we present a calculation of Post's escape function η for an infinite slab geometry. This function is needed for Post theory calculations of escape factors and effective radiative rates in that geometry.

ANALYSIS

In a recent article appearing in this journal,¹ Romberg and Kunze reported experimental studies of radiation trapping on the resonance lines of lithium and sodium for optical densities in the range $0.2 \leq k_0 l < 60$. These measurements complement previous studies of radiation trapping on the sodium resonance lines by Kibble et al² (covering the range $k_0 l < 16$) and by Huennekens and Gallagher³ ($8 < k_0 l < 800$). Romberg and Kunze carried out measurements on lithium and sodium in an atomic beam, in addition to cell measurements on sodium. Their measurements confirm the main features of the diffusion model of Milne⁴ at low optical densities, in agreement with the findings of Kibble et al, and are consistent with the Holstein theory results^{5,6} at higher opacities ($4 < k_0 l < 50$). In this discussion, k_0 is the line-center absorption coefficient and l is a geometry-dependent length parameter (l is equal to either the radius of a cylinder R or half the thickness of a slab $L/2$).

The purpose of the present article is to discuss the effects of incomplete frequency redistribution on radiation trapping in sodium vapor. In particular, we want to address the conclusion of Romberg and Kunze¹ that the Holstein theory results must be modified to take into account partial frequency redistribution for optical densities > 50 under their experimental conditions. Experimentally, this conclusion of Ref. 1 is based upon an upturn in their measured escape factor g_{eff} with increasing density when $k_0 l \geq 50$. This upturn can only be seen clearly for the two highest density data points of their sodium atomic beam experiments (see their Fig. 6 or Fig. 1 of the present article). Their lithium data did not extend to high enough density to produce similar effects. However, they state in reference to the upturn in the sodium atomic beam data, that "The escape factor reaches a minimum and increases again with increasing optical depth. Because of these at first surprising results, the same investigations were also performed in the Na resonance cell: the results were similar." Although this statement is not corroborated by the sodium cell data presented in their Figs. 5 and 6, which do not show any significant deviation from the $\sim n^{-1}$ dependence predicted by Holstein (here n is the atom density), the statement is justified by other less accurate data not reported in their paper.⁷ Unfortunately, the authors did not take further data at higher densities.

On the other hand, Huennekens and Gallagher³ have reported measurements of escape factors in a sodium cell experiment over the opacity range $8 < k_0 l < 800$. Their results are in excellent agreement with the Holstein theory predictions over the full range. In particular, over the density range between 4×10^{12} and $7 \times 10^{13} \text{ cm}^{-3}$, they observed that $g_{\text{eff}} \propto \{k_0 l [\ln(k_0 l)]^{1/2}\}^{-1}$, as predicted by Holstein (the log term is so slowly varying that this relation roughly yields $g_{\text{eff}} \propto n^{-1}$). This dependence is also identical to that seen by Romberg and Kunze for all of their cell data between 2×10^{11} and $2 \times 10^{12} \text{ cm}^{-3}$ and by all of their atomic beam data for which $k_0 l \geq 4$, with the exception of the last two points. We therefore suspect that these two data points may represent an experimental artifact.

On the theoretical side, it is true that the Holstein theory assumes complete frequency redistribution, which is not justified under all conditions. The Holstein-theory calculations assume either a purely Doppler-broadened or a purely pressure-broadened line. While complete redistribution is a very good approximation in both of these cases, every spectral line is a convolution of Doppler, pressure and natural broadening. The Holstein theory is unable to handle natural broadening because in that case complete redistribution is a very poor approximation.

Despite the fact that all three broadening mechanisms are always present, it has been shown that, in most situations, one or another of the mechanisms will dominate the trapping problem. In particular, the important mechanism is the one which dominates the line profile in the region near the unity optical depth point (i.e., near $k_0 l = 1$). The reason is that, closer to the line center, the optical density is so high that the photon is reabsorbed after travelling a very short distance regardless of the details of the lineshape, while the emission probability is small farther from the line center. This is the same reason that the emission from a self-reversed line peaks strongly near the unity optical depth points.

To quantify these arguments, Payne et al⁸ developed the following criteria for determining when complete redistribution is not a good approximation:

$$P_C = \Delta v_C / (\Delta v_C + \Delta v_N) < 0.7, \quad (1)$$

$$k_0 l [(\Delta v_N + \Delta v_C) / \Delta v_D] (\ln 2)^{1/2} > 1. \quad (2)$$

Here, Δv_C , Δv_N , and Δv_D represent the Lorentzian collisional-broadening half-width, the Lorentzian natural-broadening half-width, and the Gaussian Doppler half-width, respectively. These criteria can be interpreted as follows: inequality (1) shows that complete redistribution is a good approximation when the Lorentzian wings are dominated by collision broadening, i.e., when $P_C > 0.7$. According to inequality (2), complete redistribution is a good approximation when Doppler broadening dominates the unity depth part of the line profile, regardless of the type of broadening that dominates the Lorentzian wings of the line.

Romberg and Kunze justify their conclusion that incomplete redistribution is important at $k_0 l \sim 50$ in their experiments by appealing to these criteria and pointing out that the inequality (1) is satisfied in their case. However, both criteria must be satisfied for incomplete redistribution to be important (see, e.g., Payne et al⁸). It should be noted, for instance, that the inequality (1) is always satisfied at low densities since Δv_C is proportional to density. Thus, if inequality (1) alone invalidated the complete redistribution approximation, one would expect that the Holstein theory would break down at lower and not at higher densities.

Payne et al⁸ argue that, even if complete redistribution is not valid [i.e., even if both inequalities (1) and (2) are satisfied], the Holstein theory, where all effects associated with natural broadening are ignored, will still be valid unless

$$x_L > x_C - 0.5. \quad (3)$$

Here, x_L is the frequency at which $k_0(x_L)l = 1$ {which is given by $x_L = [\ln(k_0 l)]^{1/2}$ } and x_C is the point on the wings where the Gaussian component equals the natural Lorentzian component {i.e., $\exp(-x_C^2) = (\Delta v_N / \Delta v_D) [\ln(2)/\pi]^{1/2} x_C^2$ }. Frequencies are given here in terms of $x = (m/2kT)^{1/2} (v - v_0)\lambda$. The inequality (3) shows that natural broadening effects on radiation trapping are insignificant provided that the natural wing is small compared to the Doppler wing at the critical frequency, x_L . Because there is no frequency redistribution in the case of pure natural

line-broadening and because the scattering is effectively instantaneous, it is more accurate simply to ignore $\Delta\nu_N$ than to add it to $\Delta\nu_C$ in the Holstein pressure-broadening formulae (see also Ref. 9). Inequality (3) is roughly equivalent to (2) but is slightly more restrictive.

Applying the criteria of Payne et al to the cell experiment of Romberg and Kunze, where $l = 2.6$ cm, we find that inequality (1) is satisfied for $n < 3.1 \times 10^{14} \text{ cm}^{-3}$, inequality (2) for $n > 1.2 \times 10^{13} \text{ cm}^{-3}$, and inequality (3) for $n > 1.3 \times 10^{13} \text{ cm}^{-3}$. Thus, one would expect to see significant deviations from the Holstein theory results only in the range $1.3 \times 10^{13} < n < 3.1 \times 10^{14} \text{ cm}^{-3}$.

The data of Huennekens and Gallagher, or more recently the mercury data of Post et al,^{10,11} show clearly the transition from trapping dominated by the Doppler core to trapping dominated by the Lorentzian wings. According to the Holstein theory, the former region will show roughly an n^{-1} dependence, while the latter will be independent of density for self-broadening. The effects of incomplete redistribution are expected to manifest themselves, if at all, in just this transition region, where the unity optical depth point has just entered the Lorentzian wings, but where the density is still low enough so that $\Delta\nu_N > \Delta\nu_C$ (see Figs. 1 and 2). While Huennekens and Gallagher did not see any effects of incomplete redistribution in the sodium case where the density range of validity of both inequalities (1) and (2) is small and where hyperfine effects tend to also redistribute frequency, Post and coworkers did see such an effect in the transition region in mercury.^{10,11} It is somewhat misleading that Romberg and Kunze translated Post's data by two orders of magnitude in density, since the minimum in the escape factor vs density curve seen by Romberg and Kunze near 10^{12} cm^{-3} is nowhere near the Doppler to Lorentzian transition region

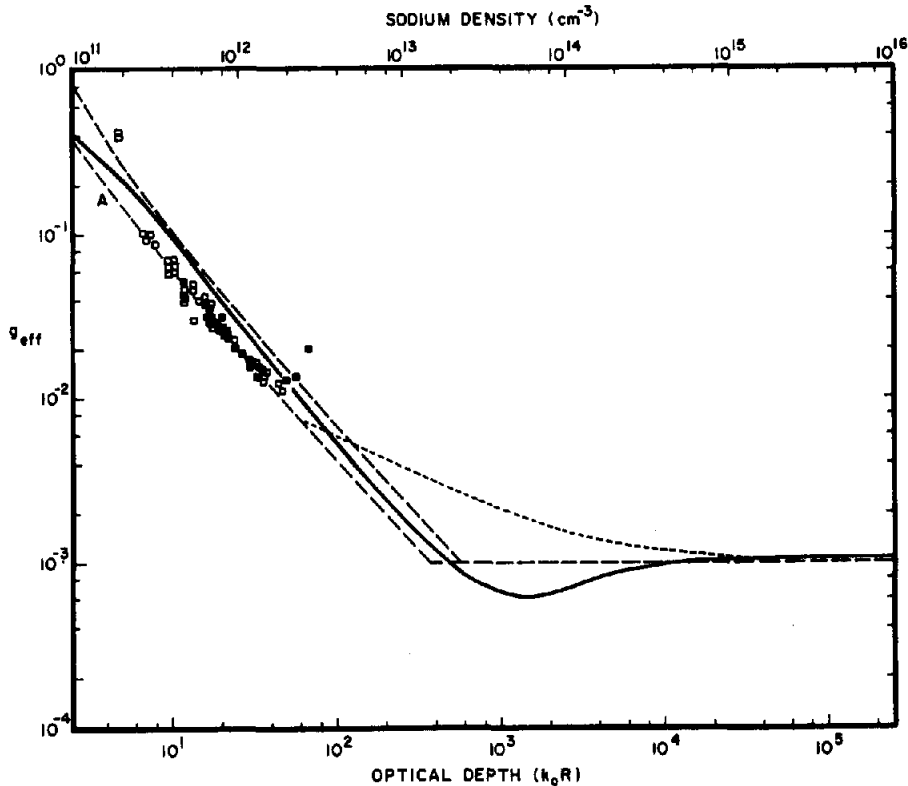


Fig. 1. The escape factor g_{eff} vs the sodium density and optical depth $k_0 l$ for the sodium D_2 line. The experimental points are from Ref. 1; \square represents data taken in a cylindrical cell of radius 2.6 cm (plotted against both density and opacity) while \blacksquare represents data taken from an atomic beam (plotted against opacity only). The solid line represents Post-theory calculations. The long dashed line represents Holstein-theory calculations, where the natural-broadening contribution to the lineshape is ignored (curve A is based on $k_0/n = 9.65 \times 10^{-12} \text{ cm}^2$, which ignores hyperfine structure, while curve B is based on the actual peak absorption cross section $k_{\text{max}}/n = 6.2 \times 10^{-12} \text{ cm}^2$). The short dashed line represents the Holstein results if $\Delta\nu_N$ is simply added to $\Delta\nu_C$ in the Holstein pressure-broadening formula. All theoretical calculations were carried out for an infinite cylinder of radius 2.6 cm.

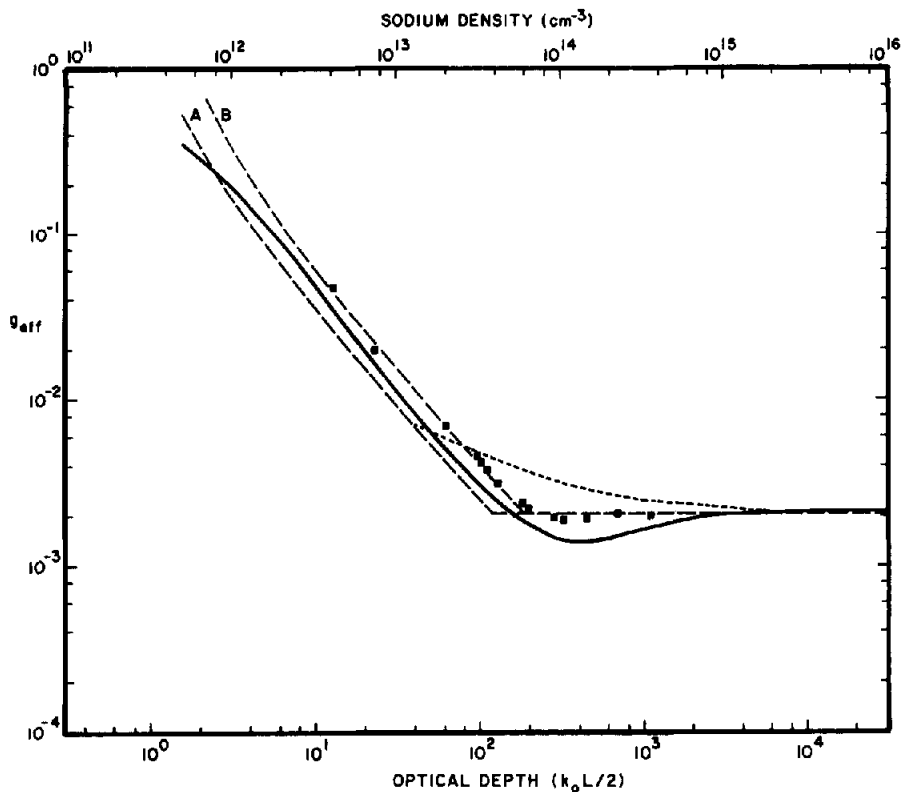


Fig. 2. The same as in Fig. 1, except that the experimental data are those of Ref. 3 which were measured in a slab geometry of thickness $L = 0.635$ cm. All theoretical calculations were carried out for an infinite slab of thickness 0.635 cm.

($\sim 1.5 \times 10^{13}$ cm^{-3} in their sodium experiment and $\sim 10^{14}$ cm^{-3} in the mercury experiment) where Post et al^{10,11} found the minimum in the g_{eff} vs density curves.

In the argument above, geometry effects can also be important (i.e., incomplete redistribution will become important at lower densities as the cell size increases). However, for small cells such as those used in Refs. 1–3, such effects will not significantly alter these conclusions.

To further investigate the effects of incomplete redistribution in the sodium case, we have carried out calculations of the escape factor g_{eff} for the sodium D_2 line as a function of density and opacity using three different methods. The results of these calculations are shown in Figs. 1 and 2, where they are compared to the measurements of Romberg and Kunze¹ and Huennekens and Gallagher,³ respectively. In both figures, the escape factor is plotted against opacity ($k_0 R$ for the cylinder and $k_0 L/2$ for the slab) as well as against sodium density. In Fig. 1, however, the density scale refers only to the cell data of Ref. 1. The beam data of Ref. 1 are plotted against opacity alone, since the effective escape distance was different in the beam and cell experiments. Due to collisional mixing between the $^2P_{1/2}$ and $^2P_{3/2}$ states at the higher densities of Ref. 3, the measured radiative decay rate ω_- is actually a linear combination of the decay rates for the two states. This was deconvolved using the ratio of escape factors for the two states taken from the Holstein theory^{5,6} and the collisional mixing rate from Ref. 12. The $^2P_{3/2}$ escape factor is smaller than the measured total decay rate by an amount ranging from 0 to 20%.

The three methods of calculating the escape factor in Figs. 1 and 2 are described in the following paragraphs. The calculations of Fig. 1 were carried out for a cylinder of radius 2.6 cm appropriate to the cell measurements of Ref. 1. The calculations of Fig. 2 were carried out for a slab of thickness 0.635 cm, as was used for the measurements of Ref. 3. The self-broadening rate for the sodium D_2 line was taken from Ref. 12.

Method 1, shown as a short dashed line, is based on the Holstein theory,^{5,6} but includes the effects of natural broadening by simply adding $\Delta\nu_N$ to $\Delta\nu_C$ in the pressure broadening formula. The escape factor is taken to be the larger of the two values calculated from the Doppler and

pressure-broadening formulae. This method is therefore based on an assumption of complete frequency redistribution for the natural as well as the Doppler and collisional-broadening contributions. It has been well established that this method fails to accurately predict the escape factor in the region where the natural wings are important (see Ref. 8 for example). The present comparisons also support this conclusion.

In the second method (long dashed line), we calculate the escape factor using either the Holstein Doppler or pressure-broadening formula (whichever yields the larger value), and ignore all effects of natural broadening on the lineshape. This empirical approach was found to give good agreement between calculated and measured escape factors in Refs. 3 and 9. However, some ambiguity exists over the correct method for incorporating hyperfine structure into the Holstein theory calculations. If the hyperfine splitting is small compared to the line width, the hyperfine structure can be ignored. In that case, the line center optical depth can be calculated from the standard formula

$$k_0 l = (2/\Delta\nu_D)[(\ln 2)/\pi]^{1/2}(\lambda^2/8\pi)(g_2/g_1)n l A_{21}, \quad (4)$$

which can be found in Mitchell and Zemansky¹³ (p. 100). This formula, which yields $k_0/n \sim 1 \times 10^{-11} \text{ cm}^2$ for the sodium D_2 line, was used in Refs. 1 and 2 to calculate Holstein theory escape factors. Calculations based on this value of $k_0 l$ are plotted as dashed curves labeled A in Figs. 1 and 2 of the present work. However, these calculations overestimate the actual trapping which is reduced by the hyperfine structure. For two hyperfine components split by a distance which is large compared to their line widths, the Holstein theory predicts that, for $k_0 l = 15$ (appropriate to the 0.635 cm slab geometry and a density of $5 \times 10^{12} \text{ cm}^{-3}$), g_{eff} will be ~ 2.35 times larger than for a single component line. This ratio shifts to ~ 2.2 when $k_0 l = 50$. When the hyperfine splitting is comparable to 1 Doppler width, as in the case of the sodium ground state, the situation is complicated. In Ref. 3, we found that a good match between theory and experiment could be obtained in the sodium case if we replaced the line-center absorption cross-section k_0/n by the peak absorption cross-section of the hyperfine doublet, $k_{\text{max}}/n \sim 6.2 \times 10^{-12} \text{ cm}^2$, in the Holstein expressions. Calculations based on this approximation are plotted as dashed lines labeled B in Figs. 1 and 2. More will be said about the hyperfine structure later.

Finally, we used the Post theory¹⁰ to calculate sodium escape factors, including the effects of incomplete redistribution and hyperfine structure (solid curves in the figures). The Post theory calculations take account of the full Voigt lineshape rather than approximating the lineshape as either a pure Gaussian or a pure Lorentzian. At first, we carried out the Post theory calculations of Fig. 1 using an approximate expression for the escape function $\eta(x) = (0.7\tau^2 + 1)^{-1}$ [where $\tau(x)$ is the optical depth at frequency x], which was mentioned in Ref. 10 as being in agreement with the exact values of η to within 30% at all τ . Unfortunately, the largest errors in this approximate η occur in the most critical region near $\tau = 1$. Therefore, we read values of the exact cylinder η function from Fig. 6 of Ref. 10 and fit them to an analytic expression $\eta = 1 - 0.0684\tau^{0.2} + 0.8332\tau^{0.4} - 1.4728\tau^{0.6} - 0.4829\tau^{0.8} + 0.6369\tau$ for $\tau < 3$. For $\tau \geq 3$, we used $\eta = (0.7\tau^2 + 1)^{-1}$ as above. These functions reproduce η to within 10% everywhere and to within 5% over the critical region $0.5 \leq \tau \leq 2.0$.

For Fig. 2, it was necessary to carry out Post theory calculations for an infinite slab geometry in order to compare to the experimental results of Huennekens and Gallagher. Post showed that besides replacing the cylinder radius R by half the slab thickness $L/2$, the only required geometry-dependent modification to his Eq. (20) for the escape factor occurs in the escape function η , which is given in the general case by

$$\eta(\rho, \tau) = 1 - \int_{\text{vol}} d\rho' \frac{\tau \exp(-\tau|\rho' - \rho|)}{4\pi|\rho' - \rho|^2} f(\rho'), \quad (5)$$

where the integral is over the slab volume. Here $f(\rho)$ is the spatial distribution of excited atoms normalized to unity at the midplane. For an infinite slab, $f(\rho)$ is only a function of the distance z from the midplane. Following Post's treatment of the cylinder, we used the fundamental mode

Table 1. Coefficients of the expansion

$$f_D(z) = \sum_{n=0}^4 A_n z^{2n}$$

for van Trigt's¹⁴ excited-atom fundamental-mode spatial distribution function appropriate to an infinite slab geometry and a Doppler lineshape. The function is normalized to $f_D(0) = 1$.

A_n	A_0	A_1	A_2	A_3	A_4
Numerical value	1.0	-0.7398	-0.4988	1.1416	-0.8326

spatial distribution $f_D(z)$ appropriate for a pure Doppler lineshape (see Ref. 10). This function was taken from van Trigt,¹⁴ who tabulated coefficients of the expansion

$$f_D(z) = N (1 - z^2)^{1/2} \sum_m a_m U_m(z) \quad (6)$$

for the slab geometry. Here $U_m(z)$ are Tschebyscheff polynomials of the second kind,¹⁵ and N is the normalization factor required to make $f_D(0) = 1$. We fit the first five terms of this expansion to a more convenient power series

$$f(z) = \sum_{n=0}^4 A_n z^{2n}. \quad (7)$$

The coefficients A_n are given in Table 1. Finally, following Post, we made the approximation that $\eta(z, \tau)$ could be evaluated at the midplane, $\eta(z, \tau) \sim \eta(0, \tau) \equiv \eta(\tau)$. This function was computed numerically and is plotted in Fig. 3. For $\tau \geq 2$ the function is well approximated by $\eta = (2\tau^2 + 1)^{-1}$, while for $\tau < 2$ we used the approximate expression $\eta = 1 + 0.0315\tau^{1/3} - 1.638\tau^{2/3} + 0.840\tau$. These analytic expressions reproduce η to within 7% everywhere. The escape factor, which was then calculated using Eq. (20) of Post, is plotted in Fig. 2.

From these plots, it can first of all be seen that the upturn in g_{eff} vs opacity observed by Romberg and Kunze does not appear to be the effect of incomplete redistribution predicted by Post, which

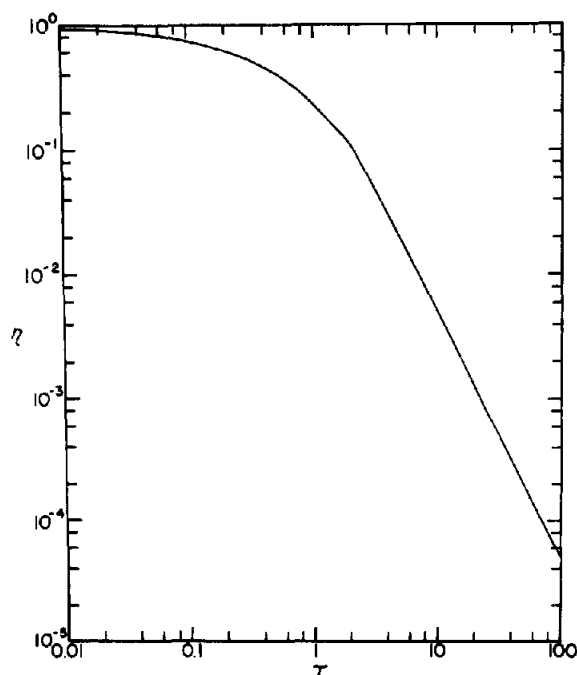


Fig. 3. Plot of Post's escape function $\eta(\tau)$ vs optical density τ for an infinite slab geometry; see Ref. 10 for definitions.

is manifested by a dip in the escape factor curve for $k_0 R \sim 10^3$. A hint of this predicted dip may, however, be evident in the data of Ref. 3 (see Fig. 2). However, the error bars in the latter experiment do not permit a conclusive statement on this point. In fact, it can be seen in Fig. 2 that in the region where the effects of incomplete redistribution are expected to be manifested, the data of Huennekens and Gallagher are more accurately reproduced by the Holstein theory (ignoring the contributions of natural broadening to the lineshape) than by the more complete theory of Post. However, we must note that whereas the effects of incomplete redistribution are small in the present case where the range of validity of both inequalities (1) and (3) is small (i.e., $1.1 \times 10^{14} < n < 3.1 \times 10^{14} \text{ cm}^{-3}$ for the conditions of Ref. 3), these effects can be quite significant under slightly different conditions (as has been demonstrated in mercury vapor by Post and coworkers^{10,11}). In the latter case, use of a more complete theory is essential.

One would expect to see agreement between the Post and Holstein theories at both low and high densities for which complete redistribution is a good approximation. This appears to be true at high densities where the detuning of the unity optical depth point from line center is large compared to the hyperfine splitting. At low densities the agreement is not good due to the *ad hoc* manner in which we have incorporated the hyperfine structure into the Holstein theory (i.e., by ignoring it as in curve A or by replacing the line center absorption coefficient k_0 by the peak absorption coefficient k_{max} as in curve B). It can be shown that the Post and Holstein theories do agree in the Doppler limit for a line without hyperfine structure (i.e., see Fig. 4 below).

To further investigate the approximations used to incorporate the sodium ground state hyperfine structure into the Holstein theory, we carried out Post theory calculations of g_{eff} for different hyperfine splittings at a sodium density of $5 \times 10^{12} \text{ cm}^{-3}$. These calculations, which were carried out for the slab of thickness 0.635 cm, are presented in Fig. 4. It can be seen that the transition in the escape factor from the case of a single unresolved line to that of two isolated lines occurs when the components are split by ~ 1 –2 Doppler widths. Under these conditions, the unity optical depth point occurs at ~ 1.2 Doppler widths. Three Holstein theory results are also given in the figure. The first is for the case of two isolated lines. The second is for a single unresolved line

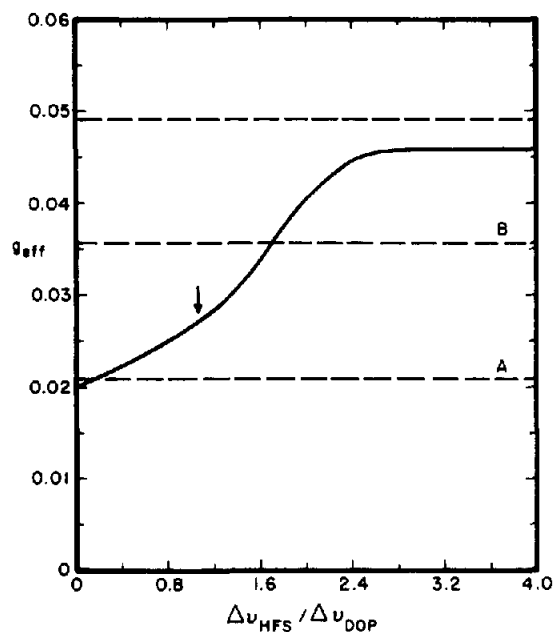


Fig. 4. Plot of the Post-theory escape factor g_{eff} for the sodium D_2 line, where the ground state hyperfine splitting was allowed to vary (solid line). The actual hyperfine splitting is shown by an arrow. Hyperfine splitting is plotted in units of the Doppler width. The calculations were carried out for a slab of thickness 0.635 cm at a sodium density of $5 \times 10^{12} \text{ cm}^{-3}$. The dashed horizontal lines represent Holstein theory results based upon the following (from top to bottom): (i) two isolated lines, (ii) a single line with peak absorption cross section $6.2 \times 10^{-12} \text{ cm}^2$ (corresponding to curves B in Figs. 1 and 2), and (iii) a single line with a line-center absorption cross-section of $9.65 \times 10^{-12} \text{ cm}^2$ (corresponding to curves A in Figs. 1 and 2).

(as used to calculate the curves labeled A in Figs. 1 and 2). The third is obtained by the replacement of k_0 by k_{\max} in the Holstein Doppler-broadening formula (curve B in Figs. 1 and 2). For the actual sodium ground state hyperfine splitting of ~ 1.1 Doppler widths at these temperatures, we can see that the Post result lies between approximations A and B.

It can be seen in Fig. 1 that the results of Ref. 1 display the n^{-1} density dependence predicted by theory over most of their range. The absolute escape factors agree well with the Holstein theory ignoring hyperfine structure (curve A). The data of Ref. 3 are more closely described by curve B. Although part of this discrepancy might be explained by the difference in geometry of the two experiments, it is clear that an unaccounted discrepancy still remains between the absolute escape factors of Refs. 1 and 3. At present, the origin of this discrepancy between the results of the two experiments is not understood, and must be attributed to some unrealized systematic error in one of the experiments.

In conclusion, we do not believe that the upturn in the escape factor vs opacity data in the sodium atomic beam experiment of Romberg and Kunze is indicative of a breakdown in the complete frequency redistribution approximation. This conclusion is based on the absence of similar observations in the cell experiments of Huennekens and Gallagher,³ and on a theoretical discussion which indicates that such effects would manifest themselves at much higher densities, if at all. In particular, the data of Huennekens and Gallagher show little, if any, indication of the effects of incomplete redistribution in this sodium case, although such effects have unambiguously been observed in mercury.¹⁰ Finally we note that under conditions where complete redistribution is not a good approximation, the recent theoretical treatments of either Post¹⁰ or Streater et al¹⁶ can be used to accurately determine radiative escape factors. In addition, as an aid to those who wish to use the Post theory to calculate escape factors, we have provided a plot in Fig. 3 of the escape function η appropriate to the infinite slab geometry.

Acknowledgements—The authors would like to acknowledge helpful discussions with Drs. J. Cooper and P. Vicharelli. We also gratefully acknowledge the financial support of GTE Laboratories Inc., General Electric Corporate Research and Development, the Energy Research Center at Lehigh University, and the National Science Foundation under grant PHY-8451279.

REFERENCES

1. A. Romberg and H.-J. Kunze, *JQSRT* **39**, 99 (1988).
2. B. P. Kibble, G. Copley, and L. Krause, *Phys. Rev.* **153**, 9 (1967).
3. J. Huennekens and A. Gallagher, *Phys. Rev. A* **28**, 238 (1983).
4. E. Milne, *J. Lond. Math. Soc.* **1**, 40 (1926).
5. T. Holstein, *Phys. Rev.* **72**, 1212 (1947).
6. T. Holstein, *Phys. Rev.* **83**, 1159 (1951).
7. H.-J. Kunze, private communication.
8. M. G. Payne, J. E. Talmage, G. S. Hurst, and E. B. Wagner, *Phys. Rev. A* **9**, 1050 (1974).
9. J. Huennekens, H. J. Park, T. Colbert, and S. C. McClain, *Phys. Rev. A* **35**, 2892 (1987).
10. H. A. Post, *Phys. Rev. A* **33**, 2003 (1986).
11. H. A. Post, P. van de Weijer, and R. M. M. Cremers, *Phys. Rev. A* **33**, 2017 (1986).
12. J. Huennekens and A. Gallagher, *Phys. Rev. A* **27**, 1851 (1983).
13. A. C. G. Mitchell and M. W. Zemansky, *Resonance Radiation and Excited Atoms*, Cambridge Press, Cambridge (1934).
14. C. van Trigt, *Phys. Rev.* **181**, 97 (1969).
15. M. Abramowitz and I. A. Stegun, *Handbook of Mathematical Functions*, p. 796, Dover, New York, NY (1972).
16. A. Streater, J. Cooper, and W. Sandle, *JQSRT* **37**, 151 (1987).